https://dx.doi.org/10.4314/ijs.v25i2.3

Ife Journal of Science vol. 25, no. 2 (2023)

GEOCHEMICAL ELEMENTS AS PROVENANCE AND PALEOENVIRONMENTAL INDICATORS IN SILICICLASTIC SEDIMENTS OF NEOGENE GWANDU FORMATION EXPOSED IN BIRNIN KEBBI AREA, NORTHWESTERN NIGERIA

Phillips, O. A.[1,2,*], Adebayo, A. J. [2], Abdulganiyu, Y.[1] and Apanpa, K. A.[2]
[1]Department of Geology, Federal University Birnin Kebbi, Nigeria.
[2]Department of Geology, The Polytechnic, Ibadan, Nigeria.
*Corresponding Author's Email: egbenzuaagaga@gmail.com
(Received: 26th March, 2023; Accepted: 23rd July, 2023)

ABSTRACT

Sediments from the exposed Gwandu Formation in Birnin Kebbi area (Northwest Nigeria) were analysed for their geochemical composition in order to determine their provenance, and paleoenvironments of deposition. Inductively Coupled plasma -mass spectrometer (ICP-MS) and -emission spectrometer (ICP-ES) were used for trace and major elements quantification. Also, samples were subjected to X-ray diffractometric analysis for the determination of their mineralogical constituents, and total sulphur (TOS) and total organic carbon (TOC) were determined using LECO analysis. High intensity of chemical weathering was inferred, as calculated values for chemical index of alteration (CIA), plagioclase index of alteration (PIA) and chemical index of weathering (CIW) were all above 90. Quartz, kaolinite, hematite and rutile in relative order of decreasing abundance, are the mineral constituents of the sediments. Bivariate plot of Fe_2O_{3T} vs MgO and the ternary diagram of MgO-Fe_2O_{3T}-SiO_2/Al_2O_3 revealed that sediments were sourced from non-marine and deltaic environments. High LREE/HREE ratios indicate relative depletion in the heavy rare earth elements (HREE), and with all values of europium anomaly below unity, it is logical to infer that sediments are predominantly constituted by felsic materials. Bivariate plot of TiO_2 vs Zr showed that approximately 93 % of the samples are dominantly felsic constituents. Also, ratios of Cr/V, Y/Ni, Th/U and the scatter plot of Th-Sc have suggested that sediments are constituted substantially by Upper continental crustal materials, and predominance of lower continental crustal components in few cases. The ratios of TOC/S suggested non-marine to marginal marine environments of deposition. Whereas, U/Th ratios implied oxic paleoenvironment for all strata, the V/Cr ratios inferred 71.43 % of the strata from Gwandu Formation were emplaced under oxidizing condition. Conversely, V/Sc ratios revealed that 78.57 % of the samples are from strata emplaced in oxygen depleted environment. Inferring from the various provenance indices, sediments of Gwandu Formation composed dominantly of materials from the upper continental crust, and low but considerable proportion from lower continental crust. Also, the application of ratios of redox sensitive elements has unveiled that sediments were emplaced principally under oxic conditions.

Keywords: Gwandu Formation, CIA, kaolinite, LREE/HREE ratios, europium anomaly, oxic paleoenvironment.

INTRODUCTION

Gwandu Formation overlies Paleogene Sokoto Group unconformably at the Southeast sector of Iullemmeden Basin, in Northwest Nigeria, where it covers almost 22,000 km^2. The unobscured litho-units are rare on the plain, but diverse on the hillsides around Birnin Kebbi and Argungu in Kebbi State where highly expressive outcrops of the formation are visible. The lithofacies were linked with deposits of Miocene-Pliocene age in Mauritania and Central African Republic, where they are referred to as the "Continental Terminal" (Kilian, 1931). Based on paleoflora (palynomorphs) constituents of the sediments, continental origin has been inferred for Gwandu Formation in Sokoto Basin (Kogbe, 1972; Salard-Cheboldaeff, 1990). The palynomorphs recovered from the Tertiary deposits, after correlation, puts the age of Gwandu Formation at Eocene-Miocene tentatively (Kogbe, 1972), whereas, subsequent work by Petters (1979) and Wright *et al.* (1985) documented Miocene-Pliocene age (Figure 1). The Central and Northern segments of Sokoto Basin present Gwandu Formation as directly overlying Kalambaina Formation, whereas, it laps over the Kalambaina, and unconformably rests on Rima and Illo Groups in the southern part of the basin. Starting from the brink at its Eastern limit at the central portion of Sokoto Basin, Gwandu Formation to the Northwest and down dip increases to approximately 1,000 feet close to Republic of Niger frontier (Kogbe, 1989).

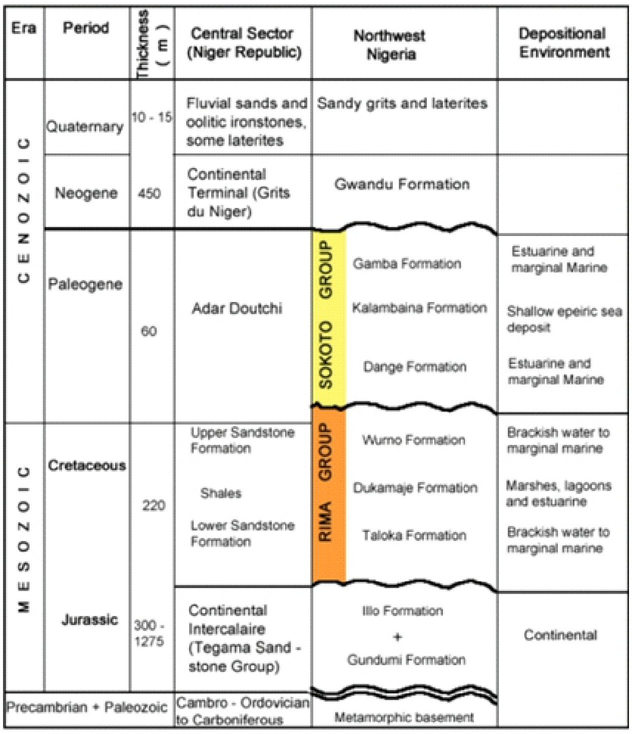

Figure 1: Regional stratigraphic subdivision of the Iullemmeden Basin (thickness and depositional environment adapted from Wright *et al.*, 1985; Petters, 1979).

Although scanty information exists on the Cretaceous and Tertiary deposits of Iullemmeden Basin, Petters (1976; 1978; 1979), Kogbe (1981; 1989; 1991), Wright *et al.* (1985), and Okosun (1999), have worked extensively on the litho- and bio-stratigraphy and tectonic history. More recent investigations on Paleogene-Neogene Formation of Sokoto Basin include hydrogeochemical /hydrochemical evaluation and characterization of groundwater (Agbede and Adegbola, 2003; Wali *et al.*, 2019; 2020), preliminary evaluation of major and trace element constituents (Bassey and Eminue, 2014), radioelement characterization (Adamu *et al.*, 2020), carbon dioxide sequestration potential (Yusuf *et al.*, 2014) and preliminary assessment of the hydrocarbon prospectivity (Obaje *et al.*, 2013). Among these investigators, Bassey and Eminue (2014) is the only available literature relevant to the study of geochemical elements as provenance signature and paleoenvironmental indicator in Sokoto Basin. It is pertinent to note, that these authors worked specifically on the upper Cretaceous to Palaeocene sediments of Sokoto Basin, whereas, the present study concentrates on the Miocene-Pliocene sediment of Gwandu Formation. Also, Bassey and Eminue (2014), focused on major elements while the trace element contents though mentioned, but not considered in the interpretation of paleoenvironment and provenance. Elsewhere in Nigeria, several researches have been undertaken on geochemistry of Cretaceous, Tertiary and Quaternary sediments with emphasis on various provenance indicator elements (Amajor, 1987; Ehinola and Abimbola, 2002; Madukwe and Bassey, 2015; Phillips *et al.*, 2017a; 2017b; Madukwe, 2019; Amiewalan *et al.*, 2020; Overare *et al.*, 2020; Ojo *et al.*, 2021).

Geochemical elements in Siliciclastic sediments have been widely used for the purposes of discriminating provenance, paleoenvironment and tectonic setting (Nesbitt 1979; Bhatia and Crook 1986; Roser and Korsch 1988; Banfield and Eggelton, 1989; Condie *et al.*, 1995; Nesbitt and Young, 1996; Li 2000; Phillips *et al.*, 2017b). It is germane to note that factors like weathering, sorting during transportation of the detrital particles, sedimentation and post-depositional diagenetic processes can influence the chemical and mineralogical composition of these sediments (Cullers *et al.*, 1979; Nesbitt *et al.*, 1997; Armstrong-Altrin, 2009). However, some light rare earth elements (LREE), heavy rare earth elements (HREE) and high field strength elements (HFSE) such as U, Th, La, Y, Sc, Cr, Th, Zr, Hf, Nb, Eu etc., and ratios like U/Th, Ni/Co, V/Sc, V/(V + Ni), V/Cr, Th/Sc have proven to be useful indicators of provenance and paleoenvironment. Their utilization as veritable tools for discrimination of provenance, paleoenvironment and tectonic setting is consequent upon their relatively low mobility and insolubility during sedimentary processes (Taylor and McLennan, 1985; Cullers *et al.*, 1987; 1988; McLennan *et al.*, 1993). These elements show very low concentrations in natural waters and are transported almost quantitatively throughout the sedimentary process from the source rocks to sink (Condie, 1991). Major elements such K_2O, CaO, Na_2O, MgO, MnO, Fe_2O_3, Al_2O_3 and TiO_2 will be utilized in the determination of various indices to unveil the intensity of weathering in the sediments' source area. Such indices are the chemical index of alteration (CIA), plagioclase index of alteration (PIA), index of compositional variability (ICV) and chemical index of weathering (CIW) to determine the extent of the chemical weathering of the constituent minerals before and after deposition of sediments. On the other hand, the rare earth, large ion lithophiles, and high field strength elements will be employed as provenance tracers, and paleoenvironmental indicators in this study. Also, X-ray diffractometer will be used to provide information on the mineralogical composition of the sediments to complement the elements' geochemistry. Specifically, the purpose of this study is to determine the provenance and environment of deposition of the sediments of Gwandu Formation using various geochemical proxies.

Study Area

The Gwandu Formation covers over 8,500 square miles in the western third of the Sokoto Basin where well-defined clay beds are commonly thick, massive, and are white, red, or gray brown to black in colour (Kogbe, 1989). It was also documented that the sand beds are fine to very coarse, predominantly quartz containing some nodules of limonite (Anderson and Ogilbee, 1973). The low plains are underlain by sand beds and the tabular-shaped were formed by resistant clay beds and are capped with residual ironstone. The Sokoto Basin which forms the southeast sector of the lullemmeden Basin, covers an area of 65,000 km^2 bounded on the north and west by Niger Republic, and on the southwest by Bénin Republic (Anderson and Ogilbee, *Op. Cit.*). The tectono-epeirogenic Iullemmeden Basin was invaded several times by epicontinental transgressions during the Cretaceous and Paleocene. At the southeast segment (Sokoto Basin), sediments were deposited during three major phases known to include the continental Mesozoic and Cenozoic phases, with an intervening marine Maastrichtian to Palaeocene phase (Kogbe, 1972). There are four main groups in Sokoto Basin *vis-à-vis* the pre-Maastrichtian sediments of fluviatile and lacustrine origin; Maastrichtian Rima Group; Paleogene Sokoto Group and the Eocene-Miocene Gwandu Formation (Kogbe, 1989).

The pre-Maastrichtian sediments, which are unconformably underlain by the Precambrian Basement Complex belong to the Gundumi and Illo formations, extend to Niger Republic at its northern part (Figure 2). The Maastrichtian witnessed sea level rise from the Tethys in the north, and the south from Gulf of Guinea (through mid-Niger Basin) and flooded the interior of the continent. This marine transgression terminated the continental period represented by the Gundumi and Illo formations. The emplacement of the Rima Group i.e., Taloka, Dukamaje and Wurno formations that overlay unconformably the pre-Maastrichtian formations represent the second phase of deposition in this sector of Iullemmeden Basin. The Tertiary Sokoto Group consisting of Dange (oldest), Kalambaina and Gamba (youngest) formations overlies the Rima Group on a well exposed erosional plane marking the boundary between Dange and Wurno formations. The Sokoto Group are overlain disconformably by the Eocene-Miocene Gwandu Formation. This formation comprises mainly of red and mottled massive clays with sandstone intercalations.

The samples for this research were collected from the exposed Gwandu Formation around Gwandan Gaji and Goru in Birnin kebbi area, Northwestern Nigeria. The study area lies between Latitudes 12° 24'N to 12° 31'N and Longitudes 4° 10'E to 4° 20'E (Figure 3), covering an area extent of about 210 km^2, and are accessible through major and secondary roads. It is in most part, consists of gently undulating plain with an average elevation between 207 m to 232 m above sea level.

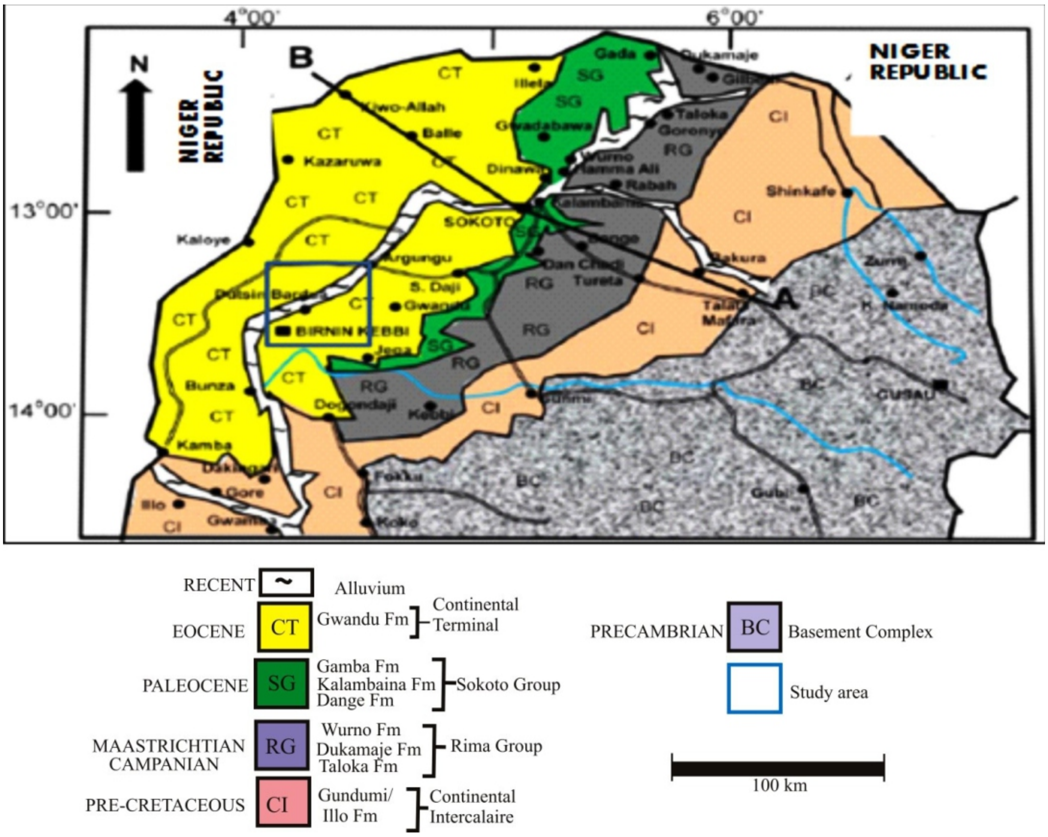

Figure 2: The geological map of the Southwest sector of Iullemmeden Basin with the lithostratigraphic position of Gwandu Formation and the study area (modified after Obaje, 2009).

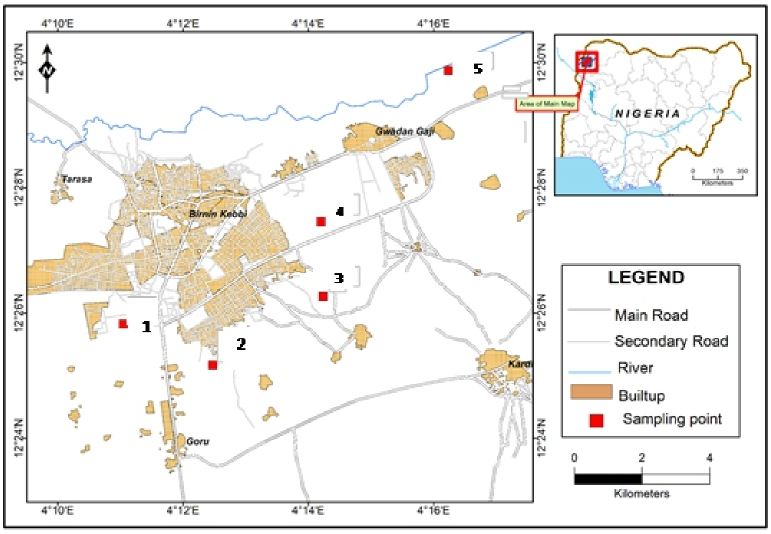

Figure 3: Map of sample locations and accessibility.

MATERIALS AND METHODS

Samples were collected from different strata of Gwandu Formation using 50 cm x 15 cm polyvinylchloride (PVC) pipes manually driven 30 cm horizontally into the beds investigated. The sediment cores were divided into two, and the first 15 cm length was kept for particle size analysis (PSA), and the other half for bulk chemical analyses. The PSA involved the use of oven-dried sample at a constant weight of 300 g in each case. Sand sizes were separated from mud by wet-sieving through a stainless-steel sieve of 63 µm aperture diameter; and 2 mm aperture sieve was used to remove gravel sized materials. The silt and clay fractions were separated by using standard pipette method of Gale and Hoare (1991).

Following the sample quartering procedure of LSASD (2000), six representative subsamples were obtained from samples collected from five locations around Gwadan Gaji and Goru in Birnin Kebbi area. The best exposure in the study area was found at Location 5, 3.0 km northeast of Gwadan Gaji where 6 representative samples from different strata were collected. Samples were also collected from the exposures at 5.0 km and 3.2 km southwest of Gwadan Gaji (Locations 3 and 4); and, 4.0 km northwest and 2.8 km northeast of Goru (Locations 1 and 2).

Sample pulverization, heat treatment, total whole rock chemical analysis, and loss on ignition (LOI) were done by Bureau Veritas Commodities Canada Ltd, Vancouver British Columbia. One hundred grams of sample was pulverized, out of which 1 g was used for LOI and 0.2 g for total whole rock characterization. Litho-geochemical technique which involved the use of 0.2 g aliquot of sample weighed into a graphite crucible and mixed with 1.5 g of lithium tetraborate flux. The crucible was placed in an oven and heated to 1050 °C for 15 min. The molten sample was dissolved in 5% nitric acid (ACS-grade HNO_3 diluted in mineralized water). Inductively Coupled Plasma-Mass Spectrometer (ICP-MS) and -emission spectrometer (ICP-ES) were employed for trace and major elements quantification in relative order, and report submitted with certificate number VAN19003415.1. LOI was calculated by weight difference after ignition at 1000 °C. Total sulphur (TOS) and total organic carbon (TOC) were determined using LECO analysis in the same laboratory. Also, representative samples were subjected to X-ray diffractometric analysis, and interpretation of diffractograms was done by comparing the peaks obtained with those obtained by the Joint Committee on Powder Diffraction Standards (JCPDS, 1980). The relative proportions of the minerals were calculated by using the area method described by Carrol (1970). The mobility of elements during chemical weathering was measured by the various indices of weathering following the procedure of McLennan (1993).

RESULTS

Result of particle size analysis (PSA)

The lowest elevation of 207 m was recorded at Location 4 compared to other locations sampled, and the dominant lithofacies are silty-clayey sand and clayey sand (Table 1). Superposition of sand and clay strata is evident at Location 5 where massive and extensive exposure of this formation is accessible. Hence, most samples were collected from this location within the elevations of 215 m to 232 m. Clayey sand forms the top-beds at the high elevation area, whereas, sandy clay facies are prevalent. The well exposed sections at Locations 2 and 3 are mainly clayey sand, variously covered at the top-surface by dispersed ironstones. The exposure at Location 1 comprises of clayey sand lithofacies with few but significant (8.0%) gravel contents at the lower bed; and top-bed as silty-clayey sand at an average elevation of 208 m. Generally, sand sized clasts dominated the study area, though with significant contents of clay and silt. In contrast, the poorly bedded but massive lower strata exposed at 3.0 km northeast of Gwadan Gaji (Location 5) are all clay beds with highly significant quantities of sand clasts. The sand size granulometry for the sand dominated lithofacies revealed overwhelming dominance of fine sand, except the lower stratum at Location 1 (GD 2) and the upper stratum at Location 4 (GD 5) which are medium sand.

Table 1: Gravel, sand, silt and clay particles distribution in sediments of Gwandu formation.

Sample Location	Sample Number	Gravel %	Sand %	Silt %	Clay %	Total %	Lithofacies Description
1. Upper bed	GD1	0.00	74.97	16.46	8.54	99.97	Clayey-silty sand, dominantly fine sand.
Lower bed	GD2	8.00	65.90	2.70	23.35	99.95	Clayey sand (with significant amount of gravel), medium sand is dominant
2. Upper bed	GD3	2.40	67.60	2.11	27.88	99.99	Clayey sand, dominantly fine sand
Lower bed	GD4	0.00	73.20	3.02	17.75	99.97	Clayey sand, overwhelming fine sand
3. Upper bed	GD5	0.00	74.90	1.90	23.15	99.95	Clayey sand, mostly fine sand.
Lower bed	GD6	0.30	57.00	3.00	39.68	99.98	Clayey sand, mostly fine sand.
4. Upper bed	GD7	0.00	79.40	9.00	11.40	99.80	Silty-clayey sand, dominantly medium sand
Lower bed	GD8	0.00	61.60	4.92	33.46	99.98	Clayey sand, mostly fine sand.
5. Bed A	GD9	0.00	74.50	3.73	21.27	99.50	Clayey sand, mostly fine sand.
Bed B	GD10	0.00	67.79	2.75	29.29	99.83	Clayey sand, mostly fine sand.
Bed C	GD11	0.00	31.40	7.84	60.30	99.54	Sandy clay
Bed D	GD12	0.00	37.75	2.96	59.28	99.99	Sandy clay
Bed E	GD13	0.45	29.50	4.94	60.01	99.90	Sandy clay
Bed F	GD14	0.00	40.50	7.80	51.60	99.90	Sandy clay

Major elements

Silica with percentages from 83.48-93.54 forms the major constituents of silty-clayey sand, clayey-silty sand and clayey sand dominating the exposed lithofacies at Locations 1 (GD 1 and 2), 2 (GD 3 and 4), 3 (GD 5 and 6), 4 (GD 7 and 8), and the upper strata at Location 5. Among the various sand lithofacies, samples collected from Location 4 contain the least average silica percentage (< 87.0%), whereas, samples from Location 5 have the highest average silica contents of over 91.0% (Table 2). The sand enriched clay beds are constituted mainly by silica (69.31% - 70.12%) and alumina (15.97% - 16.84%). In almost all samples, a decrease in alumina content was with consequential increase in quantity of silica. Similarly, low concentrations of Fe_2O_{3T} (0.92%-1.99%) and titania (0.23%-1.09%) were recorded for samples GD1 to GD10 from the sand prevalent strata. Meanwhile, much higher concentrations (Fe_2O_{3T}: 4.16%-4.99%, Titania: 1.21%-1.40%) were found in the clay dominated strata i.e., samples GD11-GD14. Interestingly, all samples collected from the exposed Gwandu Formation are depleted in CaO (0.02%-0.06%), MgO (0.02%- 0.05%), Na_2O (< 0.01%-0.03%), P_2O_5 (0.02%-0.08%), K_2O (0.02%-0.08%), MnO (<0.01%), and Cr_2O_3 (0.002%-0.013%). The total organic carbon contents are generally low (0.05%-0.16%), and the quantitative values for total sulphur are all less than 0.02% (Table 2). However, the loss on ignition is highly significant (1.50%-7.4%). The calculated CIA, CIW and PIA values are 97.23-99.39%, 99.29-99.94% and 98.57-99.76% in relative order whereas, ICV values are all greater than unity.

Table 2: Result of major elements composition for Gwandu sediments in percentage unit and their weathering indices

↓ Sample identity	SiO_2	Al_2O_3	$Fe_2O_{3(T)}$	CaO	MgO	Na_2O	K_2O	TiO_2	P_2O_5	MnO	Cr_2O_3	LOI	TOT/C	TOT/S
MDL→	0.01	0.01	0.04	0.01	0.01	0.01	0.01	0.01	0.01	0.01	0.002	-5.1	0.02	0.02
GD1	93.54	3.17	1.23	0.02	0.02	0.01	0.04	0.35	0.02	<0.01	0.002	1.50	0.05	<0.02
GD2	89.50	5.99	1.61	0.04	0.03	0.01	0.04	0.80	0.03	<0.01	0.006	1.80	0.06	<0.02
GD3	83.48	9.14	1.99	0.06	0.05	0.01	0.04	1.09	0.04	<0.01	0.010	3.90	0.07	<0.02
GD4	91.84	3.52	1.26	0.03	0.03	0.01	0.03	0.38	0.03	<0.01	0.003	2.60	0.05	<0.02
GD5	92.16	4.21	0.92	0.03	0.02	0.03	0.06	0.40	0.03	<0.01	0.004	2.10	0.05	<0.02
GD6	87.82	6.68	1.46	0.05	0.04	0.02	0.05	0.75	0.03	<0.01	0.003	3.00	0.05	<0.02
GD7	86.16	7.66	1.65	0.02	0.04	0.01	0.08	0.67	0.04	<0.01	0.012	3.50	0.09	<0.02
GD8	87.01	6.92	1.50	0.03	0.04	0.02	0.04	0.50	0.03	<0.01	0.003	3.60	0.07	<0.02
GD9	91.80	4.59	1.90	0.02	0.02	0.01	0.02	0.28	0.02	<0.01	0.003	2.20	0.06	<0.02
GD10	85.20	7.86	1.85	0.03	0.04	0.02	0.06	0.71	0.04	<0.01	0.013	4.10	0.16	<0.02
GD11	70.05	15.97	4.16	0.03	0.04	0.01	0.07	1.40	0.08	<0.01	0.013	7.00	0.06	<0.02
GD12	69.93	16.84	4.36	0.03	0.04	0.01	0.07	1.34	0.07	<0.01	0.013	7.20	0.07	<0.02
GD13	69.31	16.75	4.99	0.04	0.04	0.01	0.06	1.21	0.04	<0.01	0.010	7.40	0.14	<0.02
GD14	70.12	16.23	4.87	0.03	0.04	0.01	0.06	1.32	0.03	<0.01	0.012	7.20	0.16	<0.02
UCC values (Taylor & McLennan, 1985)	66.0	15.2	4.5	4.2	2.2	3.9	3.4	0.5	0.4	0.08	-	-	-	-

*Note MDL: Maximum detection limit

Table 2 *continued*: Result of major elements composition for Gwandu Sediments in percentage unit and their weathering indices

Sample Identity	CIA	CIW	ICV	PIA
GD1	97.84	99.69	1.44	99.05
GD2	98.52	99.83	1.87	99.12
GD3	98.81	99.89	2.27	99.24
GD4	98.05	99.72	1.47	98.87
GD5	97.23	99.29	1.16	98.57
GD6	98.24	99.70	1.74	98.96
GD7	98.58	99.87	1.89	99.61
GD8	98.72	99.71	1.71	99.28
GD9	99.03	99.89	2.03	99.46
GD10	98.62	99.75	2.10	99.36
GD11	99.32	99.94	4.40	99.75
GD12	99.35	99.94	4.59	99.76
GD13	99.35	99.94	5.23	99.70
GD14	99.39	99.94	5.10	99.75

Trace elements

The Upper Continental Crustal (UCC) values from Taylor and McLennan (1985) are widely accepted, hence, are most referenced with some confidence. Elemental concentrations in sediments below and above these values are referred to as depletion and enrichment in relative order. The concentrations in part per million (ppm) of Co (0.6-5.4), Rb (0.9-4.8) and Ni (< 20) recorded for all sediment samples collected from Gwandu Formation were below UCC values (Table 3). Samples from sand dominated lithofacies are depleted in Sc (< 11 ppm), U (< 2.8 ppm) and Th (< 10.7 ppm), whereas, clay dominated lithofacies are enriched in these elements. The comparison of geochemical and particle size data has revealed that strata with the prevalence of clay are enriched in Hf (13.9-17.4 ppm), Th (13.8-14.5ppm), U (3.1-4.3 ppm), and V (120-158 ppm). Also, enrichment of Zr, Y, La, Ce, Nd, Sm, Eu, Gd, Tb, Dy, Er, Yb, and Sc were found in the lithofacies. Sand dominated beds with highly significant clay fraction i.e., lower bed around Goru (GD2) and upper stratum at Location 2 (GD3) are highly enriched in Hf, V, Zr, Y, Ce, Pr, Nd, Sm, Eu, Gd, Tb, Dy, Er and Yb (Table 3). The ratios of LREE/HREE range from 7.1 in GD10 to 24.9 in GD1, whereas, europium anomaly varies from 0.58 in sample GD9 to 0.85 in GD3. The paleoenvironmental indices, U/Th, Ni/Co, V/Sc, V/(V+Ni) and TOT C/S range from 0.07-0.39, 1.85-16.67, 2.80-18.67, 0.74-0.94 and 5.0-16.0, respectively (Table 3).

Table 3: Result of trace elements composition in ppm unit, paleoenvironmental indices and REE ratios

↓ Sample identity MDL→	Hf	Rb	Th	U	V	Zr	Y	La	Ce	Nd	Sm	Eu	Gd	Tb	Dy
	0.1	0.1	0.2	0.1	8.0	0.1	0.1	0.1	0.1	0.3	0.05	0.02	0.05	0.01	0.05
GD1	9.4	1.4	3.4	1.3	30	375.4	9.1	147.0	25.4	9.5	1.55	0.32	1.41	0.29	1.49
GD2	16.4	2.7	10.2	2.5	112	635.1	26.8	41.8	73.1	29.8	4.90	1.01	4.58	0.74	4.53
GD3	16.1	2.6	10.0	2.6	114	634.6	26.9	41.7	72.9	30.0	4.89	1.04	4.60	0.74	4.54
GD4	9.6	1.5	3.6	1.4	29	379.1	9.0	145.0	24.8	10.4	1.62	0.42	1.39	0.31	1.51
GD5	8.6	1.7	4.9	1.1	44	332.1	9.4	28.5	54.6	24.1	3.90	0.72	2.86	0.39	1.92
GD6	8.8	1.6	4.8	1.0	45	333.2	9.7	27.6	53.9	24.3	3.87	0.76	2.88	0.38	1.93
GD7	11.3	4.8	7.9	1.9	79	449.1	16.9	36.3	66.7	29.9	5.32	1.14	4.60	0.65	3.44
GD8	10.9	4.6	7.8	1.6	82	432.1	15.9	36.6	68.0	30.1	5.38	1.13	4.58	0.66	3.41
GD9	2.9	0.9	4.1	0.3	30	126.4	6.0	29.5	40.0	15.5	2.60	0.45	2.09	0.25	1.23
GD10	2.8	1.0	4.3	0.7	28	123.5	5.7	28.9	40.2	15.6	2.59	0.47	2.10	0.23	3.71
GD11	17.2	2.8	14.0	4.3	149	668.9	30.6	83.3	150.6	62.7	11.45	2.36	9.33	1.26	6.21
GD12	17.4	2.9	13.8	4.1	158	669.1	30.2	82.5	149.7	60.9	11.03	2.38	9.36	1.31	6.20
GD13	15,9	2.4	14.4	3.1	120	633.1	21.3	59.1	99.9	36.2	5.91	1.22	4.74	0.65	3.83
GD14	13.9	2.3	14.5	3.2	121	630.2	21.6	58.9	99.6	35.9	5.89	1.24	4.72	0.68	3.82
*CI values (ppm)	-	-	-	-	-	-	1.57	0.237	0.613	0.457	0.148	0.0563	0.199	0.0361	0.246
UCC values (Taylor & McLennan , 1985)	3.8	112.0	10.7	2.8	60.0	190.0	22.0	30.0	640	26.0	4.5	0.9	3.8	0.64	3.5

Table 3 continued: Result of trace elements composition in ppm unit, paleoenvironmental indices and REE ratios

↓ Sample identity MDL→	Er	Tm	Yb	Ni	Sc	Co	Cr	Cr/V	V/Cr	U/Th	Ni/Co	V/Sc	TOT C/S
	0.03	0.01	0.05	20.0	1.0	0.2	14.0	-	-	-	-	-	-
GD1	1.06	1.17	1.22	<20	3.0	0.9	14.0	0.47	2.14	0.38	11.11	10.00	5.0
GD2	3.19	0.46	3.50	<20	6.0	1.4	41.0	0.37	2.73	0.25	7.14	18.67	6.0
GD3	3.18	0.45	3.34	<20	9.0	1.3	70.0	0.61	1.63	0.26	7.69	12.67	7.0
GD4	1.05	0.19	1.25	<20	5.0	0.8	20.5	0.71	1.41	0.39	12.50	5.80	5.0
GD5	1.17	0.17	1.21	<20	4.0	0.7	27.3	0.62	1.61	0.22	14.29	11.00	5.0
GD6	1.19	0.18	1.19	<20	7.0	0.6	20.5	0.46	2.20	0.21	16.67	6.43	5.0
GD7	1.97	0.32	2.10	<20	7.0	3.1	80.0	1.01	0.99	0.24	3.23	11.29	9.0
GD8	1.99	0.29	2.15	<20	6.0	3.0	20.5	0.25	4.00	0.21	3.33	13.67	7.0
GD9	0.71	0.10	0.62	<20	3.0	1.2	20.5	0.68	1.46	0.07	8.33	10.00	6.0
GD10	2.41	0.36	2.65	<20	10.0	1.0	90.0	3.21	0.31	0.16	10.00	2.80	16.0
GD11	3.43	0.53	3.76	<20	14.0	5.4	90.0	0.60	1.66	0.31	1.85	10.64	6.0
GD12	3.41	0.51	3.78	<20	13.0	5.2	90.0	0.57	1.76	0.30	1.92	12.15	7.0
GD13	2.43	0.38	2.68	<20	11.0	2.6	70.0	0.58	1.71	0.22	3.85	10.91	14.0
GD14	2.43	0.39	2.67	<20	12.0	2.5	80.0	0.66	1.51	0.22	4.00	10.08	16.0
*CI values (ppm)	0.160	0.0247	0.161	-	-	-	-	-	-	-	-	-	-
UCC values (Taylor & McLennan, 1985)	2.3	-	2.2	20.0	11.0	10.0				-	-	-	-

Table 3 continued: Result of trace elements composition in ppm unit, paleoenvironmental indices and REE ratios

Sample Identity	Pr	Ho	Lu	Sum LREE	Sum HREE	LREE /HREE	Eu anomaly
GD1	2.8	0.33	0.20	186.3	7.5	24.9	0.66
GD2	9.1	1.02	0.53	158.7	19.6	8.1	0.65
GD3	17.0	1.22	0.52	166.5	19.6	8.5	0.67
GD4	9.1	1.01	0.17	190.9	7.3	26.2	0.85
GD5	2.9	0.34	0.19	114.0	9.0	12.7	0.64
GD6	6.8	0.38	0.18	116.5	9.1	12.8	0.68
GD7	6.7	0.37	0.31	144.9	14.9	9.7	0.70
GD8	7.8	0.66	0.30	147.9	15.2	9.8	0.69
GD9	4.9	0.78	0.11	92.5	6.3	14.6	0.58
GD10	4.9	0.88	0.16	92.2	13.0	7.1	0.60
GD11	16.9	1.2	0.58	325.0	28.7	11.3	0.69
GD12	10.2	0.77	0.59	314.3	28.3	11.1	0.71
GD13	10.1	0.78	0.43	211.2	17.1	12.3	0.69
GD14	10.6	0.74	0.52	210.9	17.2	12.3	0.70
*CI values (ppm)	0.0928	0.0546	0.0246	-	-	-	-

*CI: Carbonaceous Chondrite values (McDonough and Sun, 1995). Europium anomaly was calculated using the formula proposed by McLennan, 1989 as $Eu/Eu^* = (Eu_{cn}) / [(Sm)_{cn} \times (Gd)_{cn}]^{0.5}$. The concentrations were normalized using chondrite values in Table 3.

Mineralogy

The main mineral phases identified by x-ray diffractometer are quartz, kaolinite, hematite and rutile. Quartz constitutes 77.61-88.50 % in the sand dominated lithofacies represented by GD1, GD3, GD5, GD7 and GD9, whereas, GD11 and GD13 contain 55.46 and 49.53 % respectively (Table 4). Kaolinite is the main clay mineral constituting 10.35-18.39 % of the samples of the sand beds and 34.34-39.49 % in samples from the clay beds. Hematite was identified in the samples, and constitutes significant proportion of 6.11-6.50 % in clay strata (GD11 and GD13), and zero to 1.15 % in sand prevalent strata (GD1, GD3, GD5, GD7 and GD9). While rutile was not identified in some samples, it however, showed significant proportion of 2.90, 1.60, 3.70 and 4.87 as percentage constituents of samples GD3, GD5, GD11 and GD13, respectively.

Table 4: Results of X-ray diffractometric analysis of samples in percentage unit from the study area.

Location	Sample Identity	Kaolinite	Quartz	Hematite	Rutile
1	GD1	11.90	88.10	0	0
2	GD3	18.39	77.61	1.10	2.90
3	GD5	12.59	85.81	0	1.60
4	GD7	10.35	88.50	1.15	0
5	GD9	12.36	86.49	1.15	0
5	GD11	34.34	55.46	6.50	3.70
5	GD13	39.49	49.53	6.11	4.87

DISCUSSION

Particle size composition

The possibility of river sediments contribution from the same and perhaps far distant source for sand dominated lithofacies were inferred for the initial deposition of sand. This may be consequent upon the overwhelming fine sand fraction in some beds and the medium sand in few cases. Subsequently, significant aeolian transport near or far from the depositional site may have produced the silt and clay fractions of the sand beds. The few but significant quantity of gravel clasts in sediments at the lower stratum of the exposure at Location 1 (GD 2) may have been contributed during peak discharge close to this location. This is possible when water is high enough to overflow its embankment under very high hydrodynamic energy. This may have taken place before the low energy fluvial and aeolian depositions in relative order. The lithofacies that are dominantly clay fraction were deposited after a substantial dissipation of hydrodynamic energy due to a long distance of transport. The information derived from particle size analysis has helped to establish that the clay beds contain significant amount of sand fractions, and sand beds are equally enriched in remarkable quantity of clay fraction. This calls for re-designation of the sedimentary strata as sandy clay and clayey sand. Corollary to this, the clay beds and sand beds are described as arenaceous and argillaceous respectively except the upper arenaceous sand beds at Location 4 being with <12 % clay fraction (Table 1). The interpretation of the various plots of geochemical elements will reliably help discern the source(s).

Major elements

The lithofacies identified from the exposed sections of Gwandu Formation are dominated by sand in some strata and clay in others. Silicon whose concentrations are well above the UCC values of Taylor and McLennan (1985) is the most predominant chemical element in the sediments. Manganese oxide is below detection limit and Na_2O contents are negligible as it shows abysmal depletion. Other soluble oxides such as CaO, MgO and P_2O_5, are highly depleted in all sediments. The depletion could be premised on the fact that continuous weathering depletes primary silicate minerals in sediments, thereby releasing cations and silicic acid into the dissolved loads of transporting fluid. This may facilitate formation of secondary minerals under favourable conditions. The chemical index of alteration (CIA), plagioclase index of alteration (PIA) and chemical index of weathering (CIW) unveiled high intensity of chemical weathering. Inferring from Nesbitt and Young (1982), the ternary plot of alumina (A), lime and soda (CN), and potash (K) employed to determine the extent of elements' mobility as defined by CIA, complemented high intensity of chemical weathering discerned (Figure 4). The ternary diagram has also shown that all samples collected from Gwandu Formation found expression in the same field as kaolinite, chlorite and gibbsite (Figure 4). The mica and feldspar constituents of granitic rocks, upon intense chemical weathering may have given up these elements during transport as ions in solution, hence, they could not be identified in the X-ray diffractograms (Figures 5a, b and c). In this case, the resulting sediments, mostly constituted by quartz, kaolinite, hematite and rutile are highly enriched in silicon and aluminium with highly remarkable depletion in mobile elements. This is evident in all the clay strata exposed at location 5 (GD 11-GD 14) with enrichment of alumina above the concentration value of the UCC of Taylor and McLennan (1985). The total iron and titania are also fairly enriched in few instances. Also, clay mineral tetrahedral sheets contain a silicon surrounded by four oxygen atoms and octahedral sheets with a metal such as Al or Mg bonded by eight oxygen atoms (Guggenheim and Martin, 1995; Yariv, 2002; Bergaya and Lagaly, 2006). Inferring from the elemental composition of the clay beds in the study area, the high depletion of Mg in sediments has given evidence of aluminium dominated octahedral sheets mostly found in kaolinite.

Samples from the strata largely dominated by clay have much higher values for loss on ignition (LOI) than those overwhelmed by sand (Table 2). Clay is mainly hydrous aluminous silicates with high cation exchange capabilities. It is therefore believed, that on ignition at 900 °C to 1,100 °C, the structural water and pore fluids in clay are released as vapour, and hence high weight loss. Considering the classification of terrigenous sandstones based on $\log(Na_2O/K_2O)$ vs $\log(SiO_2/Al_2O_3)$ from Pettijohn *et al.* (1972) with boundaries redrawn by Herron (1988), sediments collected at Locations 1-4 and upper strata of Location 5 (GD 1 to GD 10) are quartz arenites. On the contrary, the four lower strata exposed at Location 5 are classified as subarkose (Figure 6).

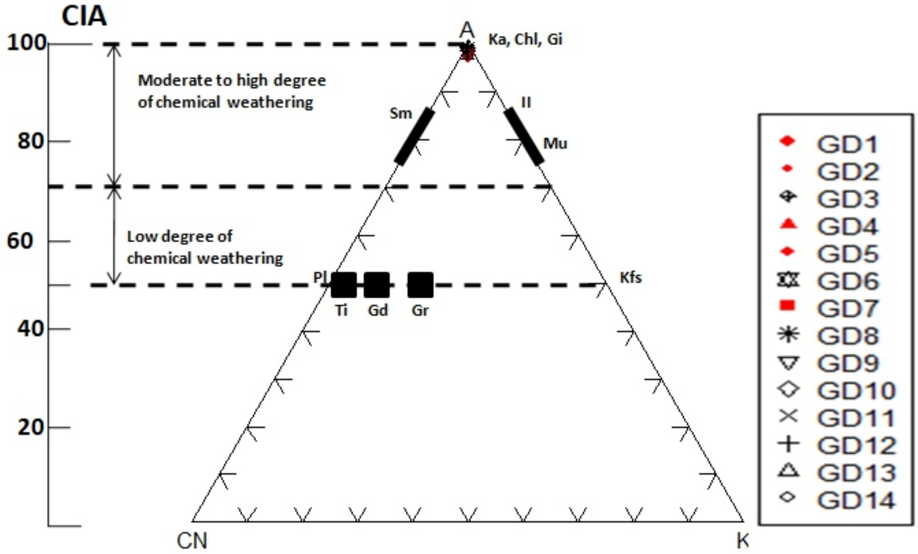

Figure 4: A-CN-K (Al_2O_3-CaO^*+Na_2O-K_2O) ternary diagram of the sample from Gwandu Formation with associated chemical index of alteration (CIA) modified from Nesbit and Young (1982). Squares and bars symbolize the average composition of tonalite (Ti), granodiorite (Gd) and granite (Gr) as well as kaolinite (Ka), chlorite (Chl), smectites (Sm), illite (Il), muscovite (Mu), plagioclase (pl), K-feldspar (kfs) and Gibbsite (Gi).

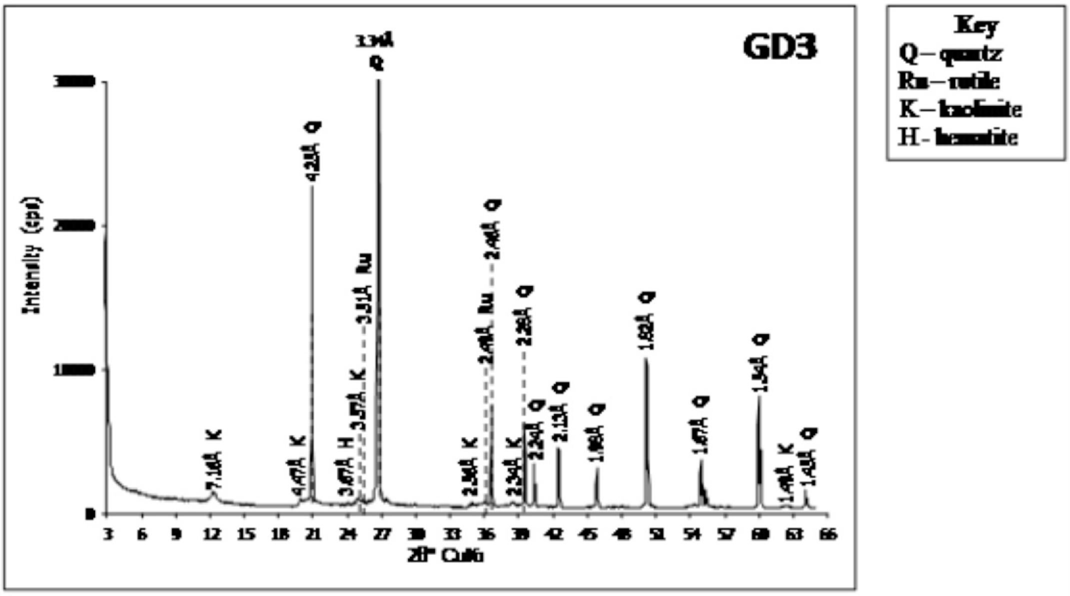

Figure 5a: X-ray diffractogram for Sample GD3.

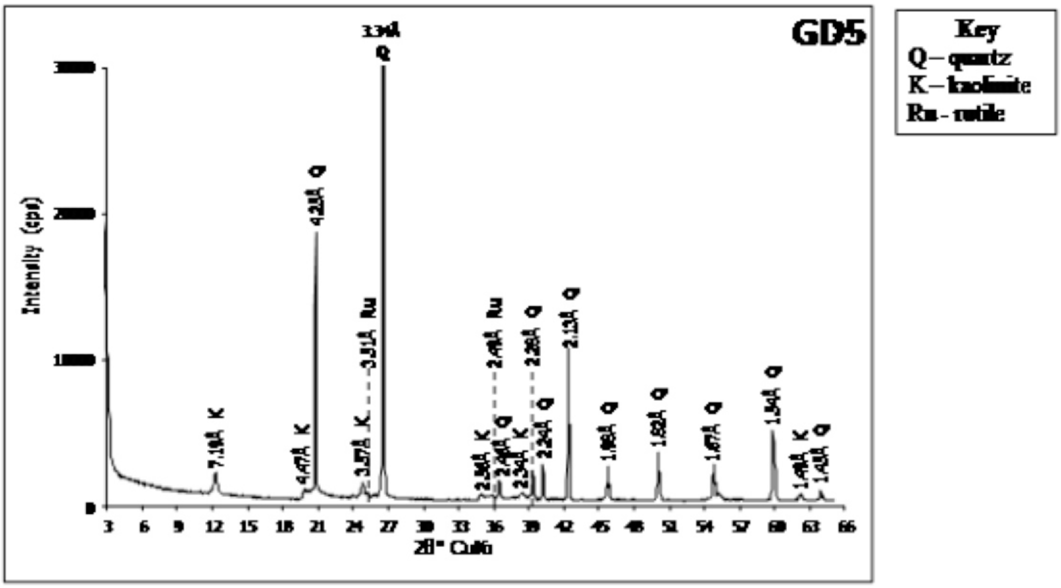

Figure 5b: X-ray diffractogram for Sample GD5.

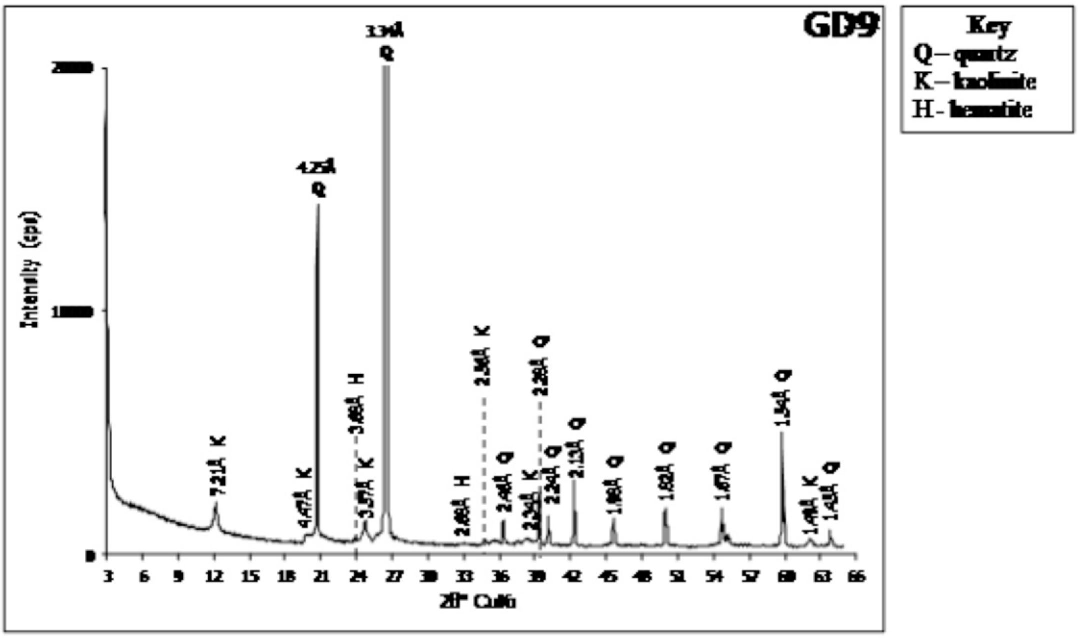

Figure 5c: X-ray diffractogram for Sample GD9.

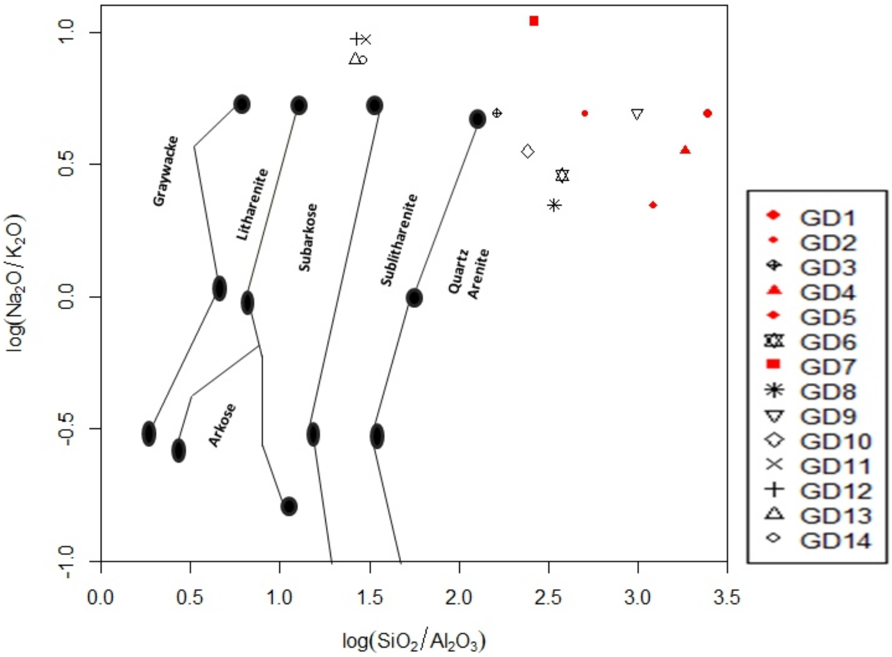

Figure 6: Classification of sediments from Gwandu Formation exposed at Birnin Kebbi area, Northwest Nigeria using Log(Na_2O/K_2O) vs Log(SiO_2/Al_2O_3) of Pettijohn *et al.* (1972) with the boundaries redrawn by Herron (1988).

The applicability of the bivariate plot of Fe_2O_{3T} vs MgO and the ternary diagram of MgO- Fe_2O_{3T}-SiO_2/Al_2O_3 (Ratcliffe *et al.*, 2007) employed to identify depositional environment has presented non-marine and deltaic sources for the sediments of Gwandu Formation (Figures 7). Despite the high intensity of weathering revealed, discerning arkosic constituents from the bivariate plot of SiO_2/Al_2O_3 vs K_2O/Na_2O (Figure 8, Creaser *et al.*, 1997) may be emphasizing granitic precursor.

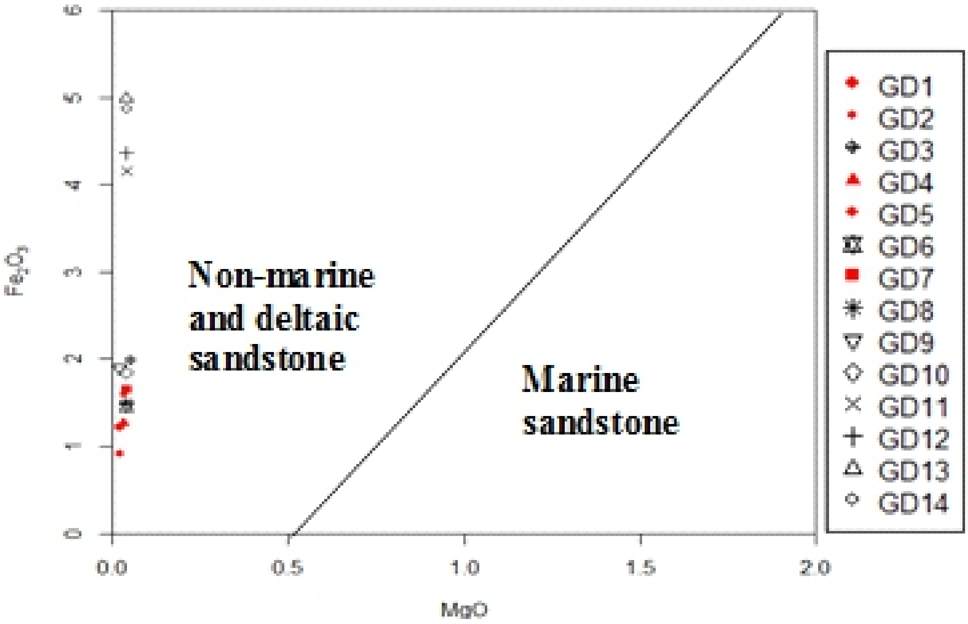

Figure 7: Binary plot of Fe_2O_3-MgO for sediments of Gwandu Formation (Adopted from Ratcliffe *et al.*, 2007).

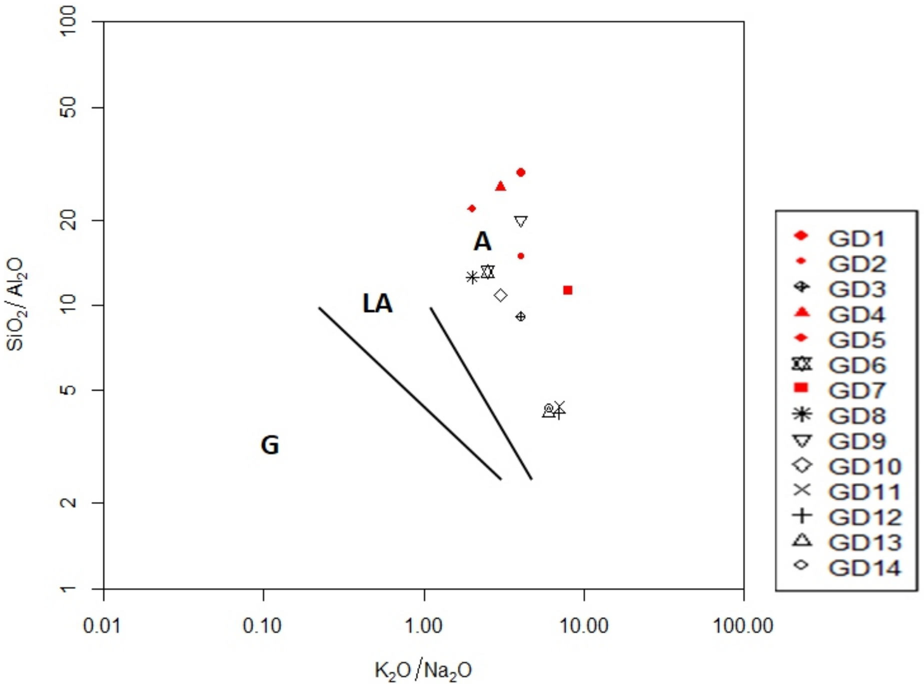

Figure 8: Chemical classification of sediments from Gwandu Formation (Modified from Creaser *et al*., 1997). G-greywacke, LA-lithic arenite, A-arkose.

Trace elements

Light rare earth elements (LREE) which are subset of the lantanide series, and are special set of transitional metals (Connelly and Damhus, 2005) showed much higher concentrations in some sediments than the UCC values of Taylor and McLennan (1985) and Condie (1993). The comparison of chondrite values for REE to the corresponding measured concentrations, also gave evidence of the higher LREE contents in sediments (La, Ce, Pr, Nd and Sm). Relative depletion is noticeable among the heavy rare earth elements (HREE). The normalized concentrations of Eu, Sm and Gd using chondrite values was used to calculate europium anomaly following the method of McLennan (1989). The resulting europium values were all below unity, hence, regarded as negative europium (Liu *et al.,* 2015). It is believed that early plagioclase crystallization from magma might have allowed reduced divalent form of europium to be incorporated into the mineral (enrichment i.e., positive europium), leaving europium depleted magma for later crystallization (negative europium). This is possible as the Ca^{2+} in plagioclase is being replaced by the divalent europium (Bau, 1991). It is important to note that the enrichment or depletion in europium is relative to other rare earth elements. In this study, the negative europium values implied sediments were sourced from felsic materials (McLennan, 1989; Liu *et al.,* 2015). Equally, the high LREE/HREE ratios is an indication of overwhelming felsic constituents in sediments of the study area. The TiO_2 vs Zr plot for the investigated sediments (Figure 9) interprets felsic igneous rocks except the sand dominated penultimate stratum (GD10) of the exposure at Gwadan Gaji area which uncloaked intermediate rocks (Hayashi *et al*., 1997; Francovschi *et al*., 2014). Trace element datasets of sediments from the exposed strata investigated were plotted on Th-Sc scatter plot in three fields (Figure 10) characterized by Th/Sc ⩾ 1.0, ⩾ 0.6-1.0, and < 0.6. These fields represent continental crust enriched in incompatible elements, andesitic composition and mafic signature in relative order. From this, it was obvious that continental signature was prevalent, while few of the representative sediments (GD10, GD6 and GD4) were sourced from intermediate igneous rocks. The ratios of Y/Ni and Cr/V have been used to discern source of sediments (Cullers, 1979; Hiscott, 1984; Cullers, 1994). The Cr/V ratio serves as an index of the enrichment of Cr over other ferromagnesian trace elements, whereas, Y/Ni presents the level of proxy for HREE. Higher Cr/V and the corresponding lower Y/Ni ratios give evidence of mafic to ultramafic source (Hiscott, 1984). In this study, abundance of felsic components has been inferred based on the prevalence of most samples with Cr/V ratios of < 2.0. Furthermore, the ratios obtained from Y/Ni (0.91-3.06) have shown that both felsic and intermediate rock-components make up the sediments, implying that upper and lower crustal materials constitute the sediments (*Cf.* Hiscott, 1984). The Th/U ratios 4.0-6.25 have suggested upper crustal composition whereas, few samples with Th/U of 2.56-3.85 are indicating lower crustal source (*Cf.* Cullers, 1994). Equally, the adoption of the crossplot of Th vs Th/U yielded well enough to permit similar interpretation (Figure 11).

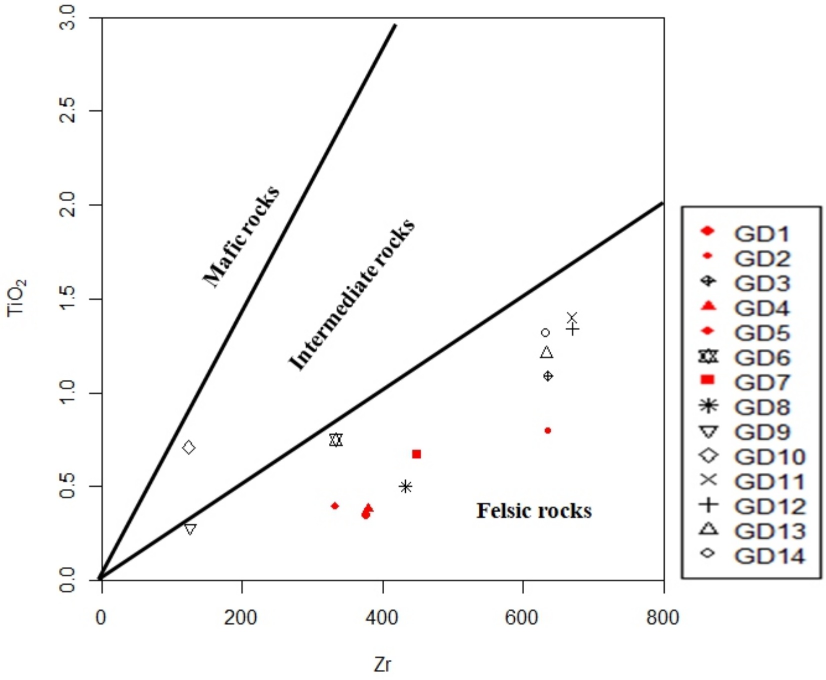

Figure 9: TiO_2-Zr plot for the exposed strata of Gwandu Formation in Birnin Kebbi area (Modified from Hayashi *et al*., 1997).

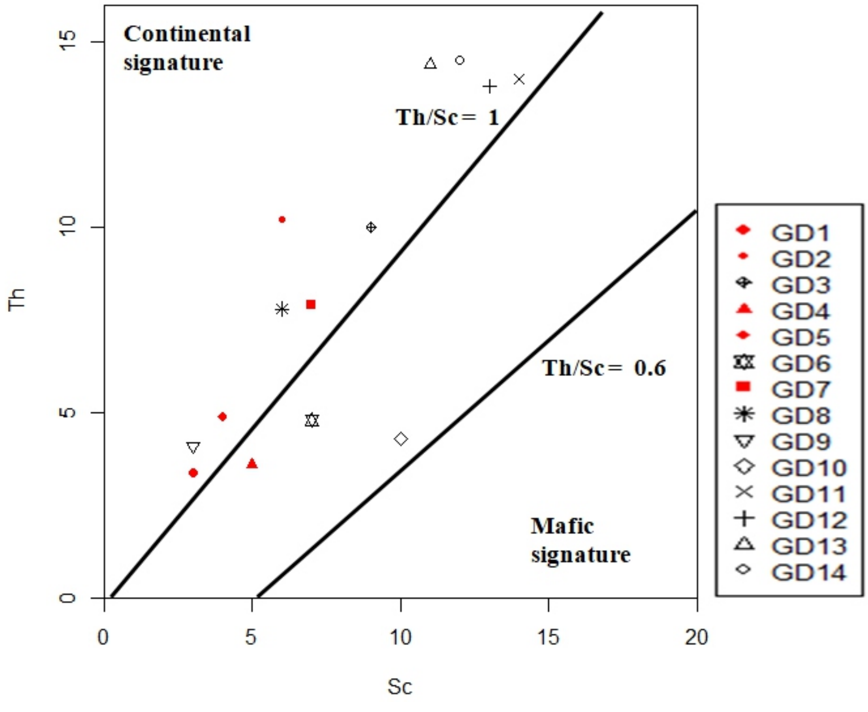

Figure 10: The scattered plot of Th versus Sc for the exposed strata of Gwandu formation.

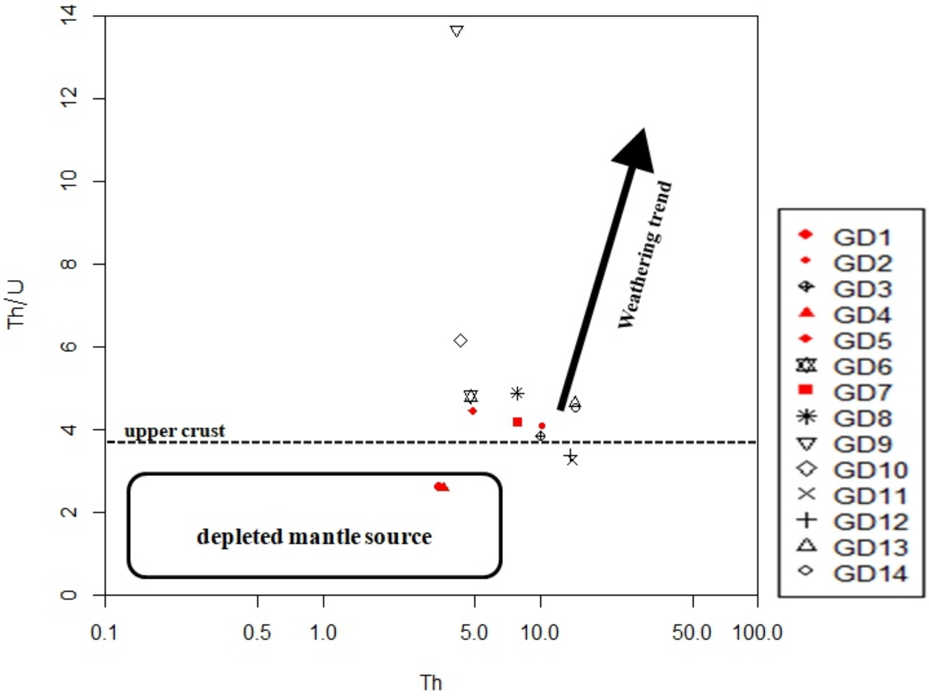

Figure 11: Discrimination plot of Th vs Th/U (Modified from McLennan *et al.*, 1993).

The TOC/S ratio has been widely used as good indicator of paleoenvironment. Hofer *et al.* (2013) proposed mean values of 4.3 ± 6.4 and 10.2 ± 13.9 for marine and non-marine environments respectively. Arising from this, non-marine to marginal marine environments has been inferred for the various regimes of sediments emplacement.

It is widely known that trace elements are sensitive to redox conditions, and the values of ratios used to characterize redox condition of environments. Redox conditions have played important role in the alteration, paragenesis and precipitation of variable-valence elements. Under oxidizing conditions, such elements occur in a high-valence state, and are easily altered unlike reducing conditions where elements occur in a low valence state and precipitated with ease. This study considered V/Cr, U/Th and V/Sc ratios as simplistic redox proxies. According to Jones and Manning (1994), V/Cr ratio higher than 4.25, < 4.25 and < 2.0 may indicate that sediments formed in anoxic, dysoxic and oxic environments respectively. The V/Cr ratios for the sediments investigated range from 0.31-4.00, implying oxic to dysoxic paleoredox conditions. The V/Cr ratios have inferred that 71.43 % of the strata from Gwandu Formation were emplaced under oxidizing condition while, others represented by GD1, GD2, GD6 and GD8 indicated dysoxic environments. The reliability of the use of Ni for paleoredox calculation in this study is in doubt because the detection limit of 20ppm is with the analytical package chosen. The U/Th ratios are all below 1.0, inferring oxic environment for the study area (Hallberg and Халлберг, 1976). Meanwhile, V/Sc ratios ascribed oxygen depleted paleoenvironment as values are greater than 9, except GD4 (5.8), GD6 (6.43) and GD10 (2.80) implying sediments were deposited under oxic conditions (Hetzel *et al.*, 2009).

CONCLUSION

The information derived from particle size composition instigated the re-designation of the sedimentary strata as sandy clay and clayey sand. Consequently, the clay beds and sand beds are arenaceous and argillaceous respectively except the upper arenaceous sand beds at location 4, being with <12 % clay fraction.

Silica is the most prevalent chemical element in the representative sediments of the exposed Gwandu Formation. Due to the intense depletion of mobile elemental oxides like Na_2O, CaO, MgO and MnO, significant relationship with relatively insoluble SiO_2 and Al_2O_3 could not be established.

This depletion has been ascribed to possible ion exchange processes and their attendant migration in solution arising from favourable chemical environment. The high enrichment of silica and alumina in sediments suggested granitic rocks as the progenitors. The ternary plot of alumina, lime and soda, and potash, as defined by CIA, complemented high intensity of chemical weathering for the studied sediments. This may hold pertinence for certain major mineral constituents (feldspar and mica) of the suggested granitic source not being identified by the x-ray diffractometer. Notwithstanding, hematite and rutile are absent in few samples, quartz, kaolinite, hematite and rutile in relative order of decreasing abundance are the mineral constituents of the sediments. The applicability of the bivariate plot of Fe_2O_{3T} vs MgO and the ternary diagram of MgO- Fe_2O_{3T}-SiO_2/Al_2O_3 revealed that sediments were sourced from non-marine and deltaic environments.

Consequent upon the LREE/HREE ratios which unveiled relative depletion in the heavy rare earth elements (HREE), and all values of europium anomaly much below unity, felsic source has been inferred for the investigated sediments. Similarly, the binary plot of TiO_2 vs Zr showed that sediments are mostly composed of felsic materials, except the lower sand bed at location 5 (GD10) which is andesitic. The Cr/V, Y/Ni, Th/U ratios and the scatter plot of Th-Sc have suggested sediments are constituted substantially by Upper continental crustal materials, and predominance of lower crustal components in few cases. The calculated ratios of TOC/S inferred non-marine to marginal marine environments of deposition. Whereas, U/Th ratios implied oxic paleoenvironment for all strata, the V/Cr ratios inferred 71.43 % of the strata from Gwandu Formation were emplaced under oxidizing condition. In contrast, V/Sc ratios revealed that 78.57 % of the samples are from strata emplaced in oxygen depleted environment. Considering the various provenance indices employed, sediments of Gwandu Formation are inferred to have been majorly contributed by materials from the upper continental crust, and complemented by small but significant proportion of lower continental crust. Also, the application of ratios of redox sensitive elements in this study, implied that sediments were emplaced principally under oxic conditions.

CONFLICT OF INTEREST

Authors declare that there is no conflict of interest.

AUTHORS' CONTRIBUTION

Phillips O.A. Conceptualisation, Methodology (Geochemistry), reviewing and editing, Adebayo A.J Software validation and original draft preparation, Abdulganiyu Y. Field mapping/sample collection, description, and pipette analysis, Apanpa K.A. Sedimentological data acquisition (including data analysis).

REFERENCES

Adamu, A., Ologe, O., Ahmed, A. L. and Sanusi, A.Y. 2020. Characterisation for Radioelements over an Escarpment Feature: a case study of the Duku-Tarasa Gwandu Ridge Area of Birnin Kebbi, NW Nigeria. *International Journal of Geosciences*, 11: 529-543.
doi: 10.4236/ijg.2020.118028

Agbede, O.A. and Adegbola, A.A. 2003. Hydrogeochemical evaluation and mechanisms controlling groundwater in different geologic environments, Western Sokoto Basin, Northwestern Nigeria. *Journal of Applied Science, Engineering and Technology,* 3: 13-18.

Amajor, L.G. 1987. Major and trace elements Petrochemistry of Albian and Turonian Shales from the Southern Benue trough, Nigeria. *Journal of African Earth Sciences*, 65: 633-641.

Amiewalan, F.O., Balogun, F.O. and Ejairu, K. 2020. Sedimentological and geochemical characterization of DF-2 well, onshore western Niger Delta: implications for provenance, tectonic history and paleo-depositional conditions. *Global Journal of Pure and Applied Sciences*, 26: 141-155.

Anderson, H.R. and Ogilbee, W. 1973. Aquifers in Sokoto Basin, Northwestern Nigeria, with a description of the general hydrology of the region. *United States Agency for International development, Geological Survey water supply*, Paper 1757-L, 88p.

Armstrong-Altrin, J.S. 2009. Provenance of sands from Cazones, Acapulco and Bahía Kino beaches, Mexico. *Revista Mexicana de Ciencias Geológicas*, 26: 764-782.

Banfield, J.F. and Eggelton, R.A. 1989. Apatite replacement and rare earth mobilization, fractionation and fixation during weathering. *Clays and Clay Minerals,* 37: 113-127.

Bassey, C. and Eminue, O. 2014. Preliminary evaluation of major and trace element contents of Cretaceous – Palaeogene Formation of the Sokoto Basin, Northwestern Nigeria. *NAFTA*, 65: 69-76.

Bau, M. 1991. Rare-earth element mobility during hydrothermal and metamorphic fluid-rock interaction and the significance of the oxidation state of europium. *Chemical Geology*, 93(3-4): 219-230. doi: 100.1016/0009-2541991)90115-8

Bergaya, F. and Lagaly, G. 2006. General introduction: Clays, clay minerals, and clay science. *Handbook of Clay Science,* Bergaya F. Theng B.K.G. and Lagaly, G. (Eds.). 1-18 Elsevier, Amsterdam. doi: 10.1016/S1572-4352(05)01001-9

Bhatia, M.R. and Crook, K.A.W. 1986. Trace element characteristics of graywackes and tectonic setting Discrimination of Sedimentary Basin. *Contributions to Mineralogy and Petrology*, 92: 181-193.

Blatt, H., Middleton, G.V. and Murray, R.C. 1980. Origin *of* Sedimentary Rocks. 2nd Ed., *Prentice-Hall, New Jersey*, 634.

Carrol, D. 1970. Clay minerals: a guide to their x-ray identification. *Geol. Soc. Am.* Special paper 126.

Condie, K.C. 1991. Another look at rare earth elements in shales. Geochim. Cosmochim. *Acta*, 55, 2527-2531. doi: 10.1016/0016-7037(91)90370-K

Condie, K.C. 1993. Geochemical composition and evolution of the upper continental crust: contrasting results from surface samples and shales. *Chemical Geology*, 104: 1–37. doi: 10.1016/0009-2541(93)90140-E

Condie, K.C., Dengate, J. and Cullers, R.L. 1995. Behaviour of rare earth elements in a paleoweathering profile on granodiorite in the front range, Colorado, USA. *Geochimica et Cosmochimica Acta*, 59: 279-294.

Connelly, N. G. and Damhus, T. 2005. Nomenclature of Inorganic Chemistry*: IUPAC Recommendations 2005*. With R. M. Hartshorn and A. T. Hutton. Cambridge: RSC Publishing. ISBN 978-0-85404-438-2.

Creaser, R.A., Erdmer, P., Stevens, R.A. and Grant, S.L. 1997. Tectonic affinity of Nisutlin and Avil assemblages strata from the Teslin tectonic zone, northern Canadian Cordillera: constraints from neodymium isotope and geochemical evidence. *Tectonics*, 16: 107–121. doi: 10.1029/96TC03317

Cullers, R. L. 1994. The controls on major and trace elements variation of shales, siltstones and sandstones of Pennsylvania-Permian age from uplifted continental blocks in Colorado to platform sediments in Kansas, USA. *Geochimica et Cosmochimica Acta,* 58: 4955-4972. doi: 10.1016/0016-7037(94)90224-0.

Cullers, R.L., Barrett, T., Carlson, R. and Robinson, B 1987. Rare earth element and mineralogic changes in Holocene soil and stream sediment: a case study in the Wet Mountains, Colorado, USA. *Chem. Geol.*, 63: 275-297. doi: 10.1016/0009-2541(87)90167-7.

Cullers, R.L., Basu, A. and Suttner, L. 1988. Geochemical signature of provenance in sand-size material in soils and stream sediments near the Tobacco Root batholith, Montana, USA. *Chem. Geol.*, 70: 335-348. doi: 10.1016/0009-2541(88)90123-4

Cullers, R.L., Chaudhuri, S., Kilbane, N. and Koch, R. 1979. Rare earths in size fractions and sedimentary rocks of Pennsylvanian-Permian age from the mid-continent of the USA. *Geochimica et Cosmochimica Acta*, 43: 1285-1301. doi: 10.1016/0016-7037(79)90119-4.

Ehinola, O. A. and Abimbola, A. F. 2002. Preliminary assessment of major and trace elements of shale in Benue Trough. *Nafta*, 53, 9: 323-326.

Francovschi, I., Grădinaru, E., Roban, R. D. and Ciobotaru, V. 2014. Geochemistry of Neoproterozoic shales from the Kalius Member: Assessing the sedimentary provenance and paleo-weathering, *Buletinul Institutului de Geologie și Seismologie al AȘM*, N2, 14-23.

Gale, J.G. and Hoare, P.G. 1991. The Physical Composition and Analysis of Regolith Materials. In Quaternary Sediments: *Petrographic Methods for the Study of Unlithified Rocks*, Belhaven Press, New York, 87-94.

Guggenheim, S. and Martin, R. T. 1995. Definition of clay and clay mineral: joint report of the AIPEA nomenclature and CMS nomenclature committees. *Clays and Clay Minerals*, 43: 255–256. doi: 10.1346/CCMN.1995.0430213

Hallberg, R.O. and Халлберг, Р.О. 1976. "A Geochemical Method for Investigation of Paleoredox Conditions in Sediments / Геохимический метод исследований условий палеоредокса в осадках", *Ambio Special Report* 4: 139-147.

Hatch, J. R. and Leventhal, J. S. 1992. "Relationship between inferred redox potential of the depositional environment and geochemistry of the Upper Pennsylvanian (Missourian) Stark Shale Member of the Dennis Limestone, Wabaunsee County, Kansas, U.S.A", *Chemical Geology* 99: 65–82. doi: 10.1016/0009-2541(92)90031-Y

Hayashi, K., Fujisawa, H., Holland, H. *et al.* 1997. Geochemistry of ~ 1.9 Ga sedimentary rocks from northeastern Labrador. *Canada:Geochimica et Cosmochimica Acta*, 61, 4115-4137. doi: 10.1016/S0016-7037(97)00214-7

Herron, M.M. 1988. Geochemical Classification of Terrigeneous Sands and Shales from Core or Log Data. *Journal of Sedimentary Petrology*, 58: 820-829. doi:10.1306/212F8E77-2B24-11D7-8648000102C1865D

Hetzel, A., Böttcher M.E., Wortmann U.G. and Brumsack, J. 2009. "Paleo-redox conditions during OAE 2 reflected in Demerara Rise, sediment geochemistry (ODP Leg 207)". *Paleogeography, Paleoclimatology and Paleoecology*, 273: 3-4, 302-328. doi: 10.1016/j.palaeo.2008.11.005

Hiscott, R. N. 1984. Ophiolitic source rocks for Taconic-Age flysch: trace elements evidence. *Geologic Society of America Bulletin*, 95: 1261-1267. doi: 10.1130/0016-7606(1984)95<1261:OSRFTF>2.0.CO;2

Hofer, G., Wagreich, M. and Neuhuber, S. 2013. Geochemistry of fine-grained sediments of the Upper Cretaceous to Paleogene Gusau Group (Austria, Slovakia): Implication for paleoenvironmental and provenance studies. *Geoscience Frontiers*, 4: 449-468. doi: 10.1016/j.gsf.2012.11.009

Joint Committee on Powder Diffraction Standards (JCPDS). 1980. Mineral powder diffraction file: vols. I and II. *Publ. Intern Centre for Diffraction Data*, Parklane, U.S.A.

Jones, B. and Manning, D. A. C. 1994. "Comparison of geological indices used for the interpretation of palaeoredox conditions in ancient mudstones", *Chemical Geology* 111: 111-129.

Kilian, C. 1931. Le principaux complexes continentaux du Sahara CR. *Soc. Géol. Fr.*, 109. doi: 10.1016/S1874-5997(97)80008-1

Kogbe, C. A. 1972. Geoogy of the Upper Cretaceous and lower Tertiary sediments of the Nigeria Sector of the Iullemmeden Basin (West Africa). *Geologisch Rundschau*, 62: 197-211. doi: 10.1016/0195-6671(81)90007-0

Kogbe, C.A. 1981. Cretaceous and Tertiary of the Iullemmeden Basin in Nigeria (West Africa). *Cretaceous Research*, Elsevier Publication, 129-186. doi: 10.1016/0195-6671(81)90007-0

Kogbe, C.A. 1989. Geology of the Southeastern (Sokoto) Sector of the Iullemmeden Basin. Monograph. 420.

Kogbe, C.A. 1991. Stratigraphy and tectonic history of the Iullemmeden Basin in West Africa. Rock Review International, Geoscience Consulting Associates, Tour Onyx, 10 Rue Vandrezanne, 75013 Paris, France.

Li, Y.H. 2000. A compendium of Geochemistry. Princeton University Press, Princeton, NJ, 475.

Liu, Y., Cheng, Y., Liu, J., Zhang, L., Zhang, C. and Zheng, C. 2015. Provenance discrimination of surface sediments using Rare Earth Elements in the Yalu River Estuary, China. *Environ. Earth Sci.* 74 (4): 3507–3517. doi: 10.1007/s12665-015-4391-x

LSASD. 2000. LSASDPROC-300-R4, Soil Sampling. *Laboratory Services and Applied Science Division, US Environmental Protection Agency*, Athens, Georgia, 29.

Madukwe, H.Y. 2019. Provenance, tectonic setting, source area weathering and paleo-redox condition of (late Cretaceous) Ise sandstone, Abeokuta group, Dahomey basin (SW Nigeria). *Bulletin de l'Institut Scientifique*, Rabat, Section Sciences de la Terre, 41: 55 – 70.

Madukwe, H.Y. and Bassey, C.E. 2015. Geochemistry of the Ogwashi-Asaba Formation, Anambra Basin, Nigeria. Implications for Provenance, Tectonic Setting, Source Area, Weathering, Classification and Maturity. *International Journal of Science and Technology*. 4, 7.

McDonough, W.F. and Sun, S.S. 1995. "The composition of the Earth". *Chemical Geology*, 120: 223-253. doi: 10.1016/0009-2541(94)00140-4

McLennan, S.M. 1989. Rare earth elements in sedimentary rocks: Influence of of provenance and sedimentary process. *Review of Mineralogy*, 21: 169-200. doi: 10.1515/9781501509032-010

McLennan, S.M. 1993. Weathering and global denudation. *Journal of Geology*, 101: 295-303.

McLennan, S.M., Hemming, S., McDaniel, D.K. and Hanson, G.N. 1993. Geochemical approaches to sedimentation, provenance and tectonics. In: M.J. Johnson and A. Basu, (Eds.), Processes Controlling the Composition of Clastic Sediments. *Geological Society of American*, Special Paper, 32: 21-40. doi:10.1130/SPE284-p21

Nesbitt, H.W. 1979. Mobility and fractionation of REE during weathering of granodiorite. *Nature*, 279: 206-210.

Nesbit, H.W. and Young, G.M. 1982. Early Proterozoic Climates of sandstone mudstone uites using SiO_2 content and K_2O/Na_2O ratio. *Nature*, 299: 715-717. doi: 10.1038/299715a0

Nesbitt, H.W. and Young, G.M. 1996. Petrogenesis of sediments in the absence of chemical weathering: effects of abrasion and sorting on bulk composition and mineralogy. *Sedimentology*, 43: 341-358. doi: 10.1046/j.1365-3091.1996.d01-12.x

Nesbitt, H.W., Fedo, C.M. and Young, G.M. 1997. Quartz and feldspar stability, steady and non-steady state weathering and petrogenesis of siliciclastic sands and muds. *Journal of Geology*, 105: 173-191.

Obaje, N. G. (2009). Geology and mineral resources of Nigeria. Lecture notes in Earth Science. *Springer Berlin,* 120. doi: 10.1007/978-3-540-92685-6.

Obaje, N.G., Aduku, N. and Yusuf, L. 2013. Preliminary Assessment of the Hydrocarbon Prospectivity in Sokoto Basin. *Petroleum Technology Development Journal*, 3: 66-80. doi: 10.4236/gep.2022.105001

Ojo, O.J., Adepoju, S.A., Awe, A. and Adeoye, M.O. 2021. Mineralogy and geochemistry of the sandstone facies of Campanian Lokoja Formation in the Southern Bida basin, Nigeria: implications for provenance and weathering history. *Heliyon*, 7, e08564. doi: 10.1016/j.heliyon.2021.e08564

Okosun, E. A. 1999. Late Paleocene biostratigraphy and palaecology (Foraminifera and Ostracode) of two boreholes in the Sokoto Basin, N.W. Nigeria. *Journal of Mining and Geology*, 35: 39-47.

Overare, B., Osokpor, J., Ekeh, P.C. and Azmy, K. 2020. Demystifying provenance signatures and paleo-depositional environment of mudrocks in parts of south-eastern Nigeria: Constraints from geochemistry. *Journal of African Earth Sciences*, 172. doi: 10.1016/j.jafrearsci.2020.103954.

Petters, S. W. 1976. The marine Maastrichtian and Paleocene sediments of Northwestern Nigeria: The Dukamaje Formation and the Sokoto Group. *Geological guide to some Nigeria Cretaceous-Recent localities*. 7th African Micropal. Coll. Ile-Ife, Nigeria, 75-87.

Petters, S. W. 1978. Maastrichtian – Palaeocene foraminifera from NW Nigeria and their paleogeography. *Acta Paleontologica Polonica*, 23: 131–150.

Petters, S. W. 1979. Stratigraphic history of the south-central Saharan region. *Geological Society of America Bulletin*, 90: 753–760. doi: 10.1130/0016-7606(1979)90<753:SHOTSS>2.0.CO;2

Pettijohn, F.J., Potter, P.E. and Siever, R. 1972. Sand and Sandstone. Plate Motions Inferred from Major Element Chemistry of Lutites. *Precambrian Research*, 147: 124-127. doi: 10.4236/oalib.1108439

Phillips, O.A., Adebayo, A.J. and Falana, A.O. 2017a. Mineralogical and Geochemical Studies of Lagos Lagoon Sediments, Southwest Nigeria: Implications for Weathering and Provenance. *Journal of Mining and Geology,* 53: 21 – 30.

Phillips, O.A., Falana, A.O. and Adebayo, A.J. 2017b. The geochemical composition of sediments as a proxy of provenance and weathering intensity: a case study of Southwest Nigeria's Coastal Creeks. *Geology, Geophysics and Environment*, 43: 229-248. doi: 10.7494/geol.2017.43.3.229

Ratcliffe, K.T., Morton, A.C., Ritcey, D.H. and Evenchick, C.A. 2007. "Whole-rock geochemistry and heavy mineral analysis as petroleum exploration tools in the Bowser and Sustut basins, British Columbia, Canada". *Bulletin of Canadian Petroleum Geology , 55*: 320–336. doi: 10.2113/gscpgbull.55.4.320

Roser, B.P. and Korsch, R.J. 1988. Provenance signatures of sandstone-mudstone suites determined using discriminant function analysis of major element data. *Chem. Geol.* 67: 119-139. doi: 10.1016/0009-2541(88)90010-1

Salard-Cheboldaeff, M.I. 1990. Intertropical African palynostratigraphy from Cretaceous to late quaternary times. *Journal of African Earth Sciences*, 11: 1-24. doi: 10.1016/0899-5362(90)90072-M.

Taylor, S.R. and McLennan, S.M. 1985. The Continental Crust: Its Composition and Evolution. Blackwell Scientific Publications, 312. doi: 10.1002/gj.3350210116.

Wali, S. U., Alias, N. and Harun, S. B. 2020. Hydrogeochemical evaluation and mechanisms controlling groundwater in different geologic environments, Western Sokoto Basin, Northwestern Nigeria. *SN Applied Sciences*, 2, 1808.

Wali, S. U., Umar, K. J., Abubakar, S. D., Ifabiyi, I.P., Dankani, I.M., Shera, I.M. and Yauri, S.G. 2019. Hydrochemical characterization of shallow and deep groundwater in Basement Complex areas of southern Kebbi State, Sokoto Basin, Nigeria. *Applied Water Science*, 9: 189.

Wright, J.B., Hastings, D.A., Jones, W.B. and Williams, H.R. 1985. Geology and Mineral Resources *of* West Africa. *George Allen* and *Unwin* Ltd., London, 35: 48-49. doi: 10.1007/978-94-015-3932-6.

Yariv, S. 2002. Introduction to organo-clay complexes and interactions. In: *Organo-Clay Complexes and Interactions*. Yariv, S. and Cross, H. (Eds.). Marcel Dekker, Inc. New York.

Yusuf, L., Obaje, N.G., Jibrin, B., Tsepav, M.T. and Liman, H.M. 2014. Overview of Lullemmeden Basin for CO_2 Sequestration Potential In North-Western Nigeria. *International Journal of Scientific and Technology Research*, 3: 3.